

Supplementary

Effects of Phosphorus in Growth Media on Biomineralization and Cell Surface Properties of Marine Cyanobacteria *Synechococcus*

Carlos Paulo ¹, Janice P. L. Kenney ^{2,†}, Per Persson ³ and Maria Dittrich ^{1,*}

¹ Department of Physical and Environmental Sciences, University of Toronto Scarborough, 1265 Military Trail, Toronto, ON M1C 1A4, Canada; carlos.fernandesesilvapaulo@mail.utoronto.ca

² Department of Chemistry, Umeå University, SE-901 87 Umeå, Sweden; janicekenney@gmail.com

³ Centre for Environmental and Climate Research & Department of Biology, Lund University, SE-223 62 Lund, Sweden; per.persson@biol.lu.se

* Correspondence: mdittrich@utsc.utoronto.ca; Tel.: +1-416-208-2786

† Current Address: Wood, Harwell Campus, OX11 0QB Oxford, UK.

Received: 31 October 2018; Accepted: 1 December 2018; Published: date

Supplementary information 1. Culture medium for cyanobacteria

ASN III with Vitamin B12- Marine strain - *Synechococcus* PCC8806

180 μ M of Phosphorus

25 mg.L⁻¹ NaCl; 2000 mg.L⁻¹ MgCl₂.6H₂O; 500 mg.L⁻¹ KCl, 750 mg.L⁻¹ NaNO₃; 40 mg.L⁻¹ K₂HPO₄.3H₂O; 3500 mg.L⁻¹ MgSO₄.7H₂O; 500 CaCl₂.2H₂O; 3 mg.L⁻¹ C₆H₈O₇; 3 mg.L⁻¹ C₆H₅+4γFexNyO₇; 0.5 mg.L⁻¹ Na-EDTA; 40 mg.L⁻¹ Na₂CO₃; 2.86 mg.L⁻¹ H₃BO₃; 1.81 mg.L⁻¹ MnCl₂.4H₂O; 222 μ g.L⁻¹ ZnSO₄.7H₂O; 390 μ g.L⁻¹ Na₂MoO₄.2H₂O; 79 μ g.L⁻¹ CuSO₄.5H₂O; 49.4 μ g.L⁻¹ Co(NO₃)₂.6H₂O; 10 μ g.L⁻¹ α -(5,6-dimethylbenzimidazolyl)cobamidcyanid (Vitamin B12)

90 μ M of Phosphorus

25 mg.L⁻¹ NaCl; 2000 mg.L⁻¹ MgCl₂.6H₂O; 500 mg.L⁻¹ KCl, 750 mg.L⁻¹ NaNO₃; 20 mg.L⁻¹ K₂HPO₄.3H₂O; 3500 mg.L⁻¹ MgSO₄.7H₂O; 500 CaCl₂.2H₂O; 3 mg.L⁻¹ C₆H₈O₇; 3 mg.L⁻¹ C₆H₅+4γFexNyO₇; 0.5 mg.L⁻¹ Na-EDTA; 40 mg.L⁻¹ Na₂CO₃; 2.86 mg.L⁻¹ H₃BO₃; 1.81 mg.L⁻¹ MnCl₂.4H₂O; 222 μ g.L⁻¹ ZnSO₄.7H₂O; 390 μ g.L⁻¹ Na₂MoO₄.2H₂O; 79 μ g.L⁻¹ CuSO₄.5H₂O; 49.4 μ g.L⁻¹ Co(NO₃)₂.6H₂O; 10 μ g.L⁻¹ α -(5,6-dimethylbenzimidazolyl)cobamidcyanid (Vitamin B12)

45 μ M of Phosphorus

25 mg.L⁻¹ NaCl; 2000 mg.L⁻¹ MgCl₂.6H₂O; 500 mg.L⁻¹ KCl, 750 mg.L⁻¹ NaNO₃; 10 mg.L⁻¹ K₂HPO₄.3H₂O; 3500 mg.L⁻¹ MgSO₄.7H₂O; 500 CaCl₂.2H₂O; 3 mg.L⁻¹ C₆H₈O₇; 3 mg.L⁻¹ C₆H₅+4γFexNyO₇; 0.5 mg.L⁻¹ Na-EDTA; 40 mg.L⁻¹ Na₂CO₃; 2.86 mg.L⁻¹ H₃BO₃; 1.81 mg.L⁻¹ MnCl₂.4H₂O; 222 μ g.L⁻¹ ZnSO₄.7H₂O; 390 μ g.L⁻¹ Na₂MoO₄.2H₂O; 79 μ g.L⁻¹ CuSO₄.5H₂O; 49.4 μ g.L⁻¹ Co(NO₃)₂.6H₂O; 10 μ g.L⁻¹ α -(5,6-dimethylbenzimidazolyl)cobamidcyanid (Vitamin B12)

The growth media were adjusted to pH 7.4 \pm 0.02 using HCl 1N under sterile conditions.

Supplementary Information 2. Biomass quantification and growth curves

Optical densities (OD) were measured spectrophotometrically at 650 nm using GENESYS 5 UV-Vis (Thermo Fisher Scientific). Total cell concentration (cells L⁻¹) was determined by epifluorescence microscopy based on the autofluorescence characteristic of phycoerythrin-pigments identified in *Synechococcus* strains. Cell enumerations were performed at a magnification of 1000x with ten random microscope fields (approximately 300 total cell counts). Cell number was determined using cellSense® imaging system of the Olympus IX 51 microscope with TRITC filter (543/22 Excitation, 593/40 Emission). Calibration curves of absorbance (OD₆₅₀) against microscope enumeration of cell numbers for the three *Synechococcus* strains were generated with R² values ranging from 0.973 – 0.997. The dry bacteria weight was determined from a bacterial pellet recovered by centrifugation and dried at 65°C for 24-48 hours until a constant weight was attained.

For determination of the growth rates, each growth curve was fitted to a Gompertz model, expressed as $f(t) = ae^{-e^{-k(x-x_c)}}$, where a is the upper asymptote of the sigmoid or the carrying capacity, k is the growth rate constant (d⁻¹), and xc the inflection point.

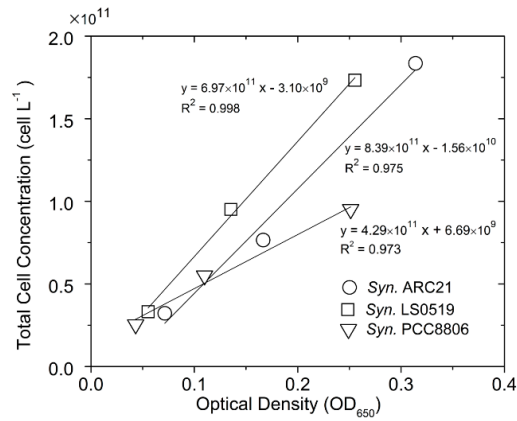


Figure S1. Calibration curves of *Synechococcus* sp. optical densities to cell enumeration by image-analyzed epifluorescence microscope

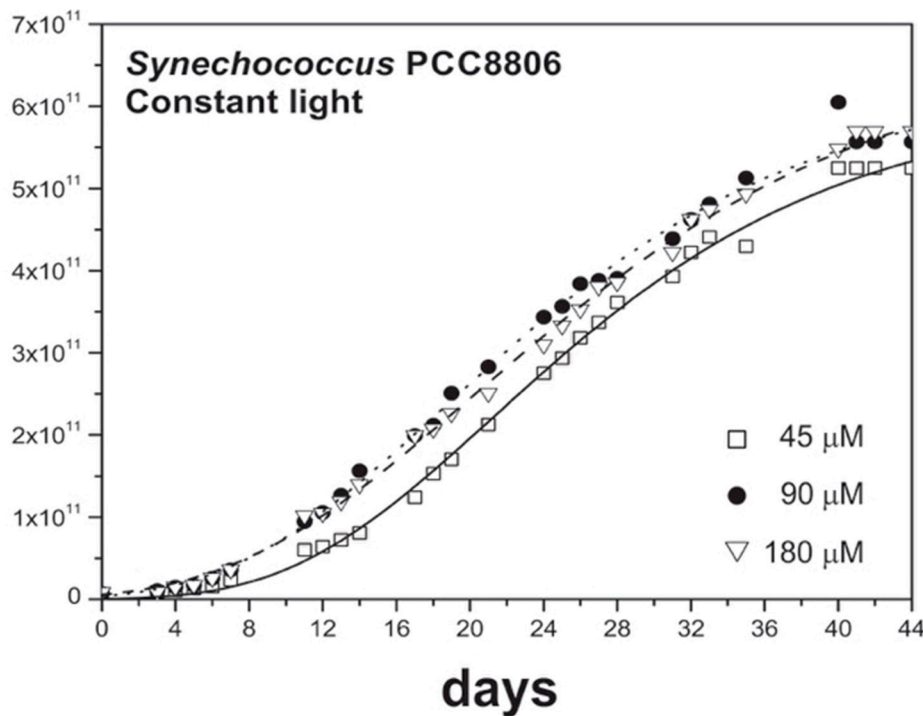


Figure S2. Growth curves of *Syn. PCC8806* under constant light. Each data point was obtained from the average of five replicates.

Table S1. Predicted carrying capacity value or the maximum microbial population reached at the stationary phase (a, as OD650 and cells.L⁻¹), specific growth rate (k, as d⁻¹) obtained from Gompertz model curve fitting. (Confidence interval (R2) of 0.99).

		Constant Light			
		P (μM)	k(d ⁻¹) ± s.d.	a	cells.L ⁻¹
Syn. PCC8806	45	0.095 ± 0.004	1.378	5.98E+11	
	90	0.077 ± 0.004	1.657	7.17E+11	
	180	0.070 ± 0.003	1.734	7.51E+11	

Supplementary information 3. Single-cell envelope thickness measurement

The thickness of single-cells ($n \geq 10$) in their stationary growth phase was measured in TEM sections. The average thickness was determined as the average distance between the outermost and innermost layer of the cell envelope assuming that both layers form two concentric circles. The two boundary layers were digitized using vector graphics editor software and define an annular geometrical region. The area and perimeter of this feature were calculated using computer-aided design tools. The average thickness of the cells envelope (\bar{t}_{env}) was estimated with the following expression:

$$\bar{t}_{env} = \frac{1}{N} \sum_{i=1}^N A_a \times (P_{\bar{a}})^{-1} = \frac{1}{N} \sum_{i=1}^N \pi(R^2 - r^2) \times (2\pi R + 2\pi r)^{-1/2}$$

where R is the external circle radius; r is the internal circle radius; A_a is the total area of the annular region; and P _{\bar{a}} corresponds to the perimeter of the mid-point of the annular region. The significance of P concentrations on the cell thickness was evaluated with one-way analysis of variance (ANOVA, p < 0.05).

Table S2. ANOVA analysis of the thickness of cell surfaces under different P conditions

Syn. PCC 8806						
Source of Variation	SS	df	MS	F	P-value	F crit
Between Groups	160.77	2	80.38	3.31	0.04	3.13
Within Groups	1677.89	69	24.32			
Total	1838.66	71				

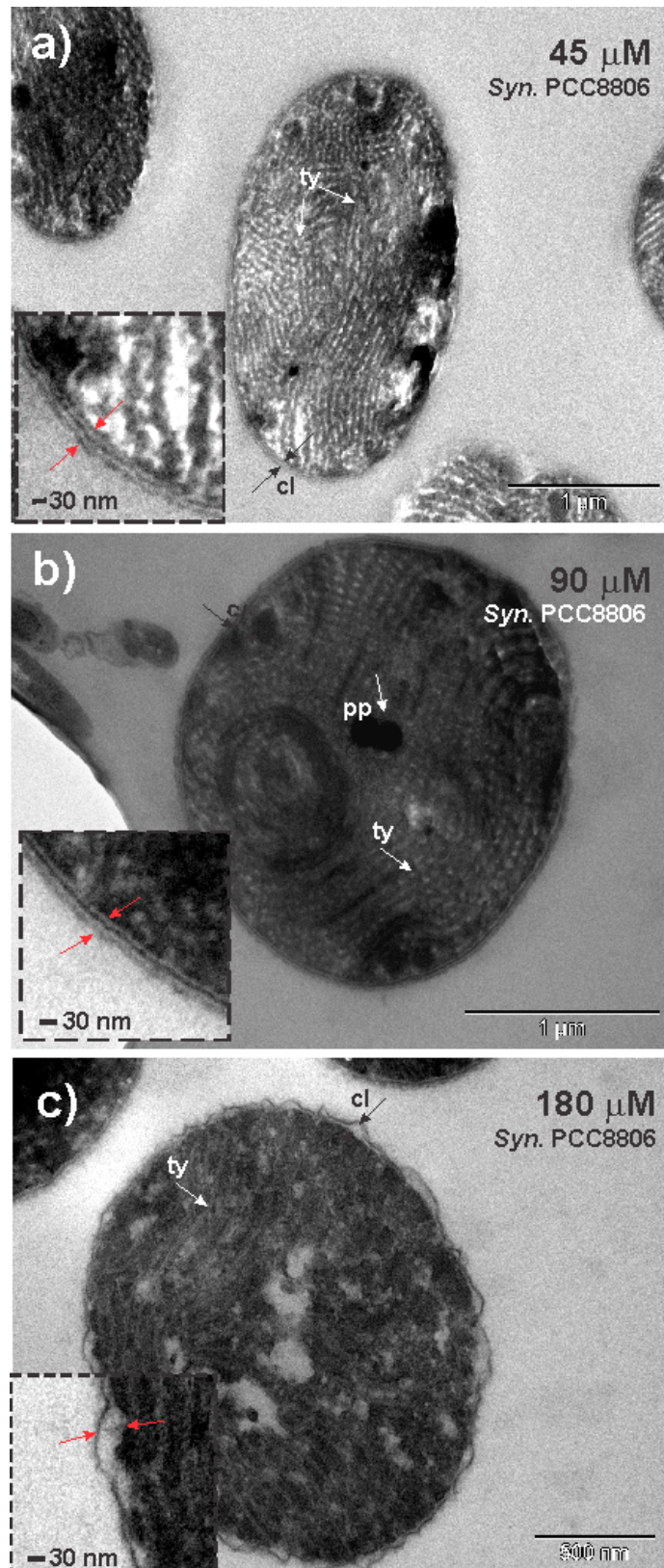


Figure S3. Example of the transmission electron microscopy (TEM) micrographs of single cells, which was used for thickness measurements. The red arrows indicate the cell membrane structure in the zoomed areas.

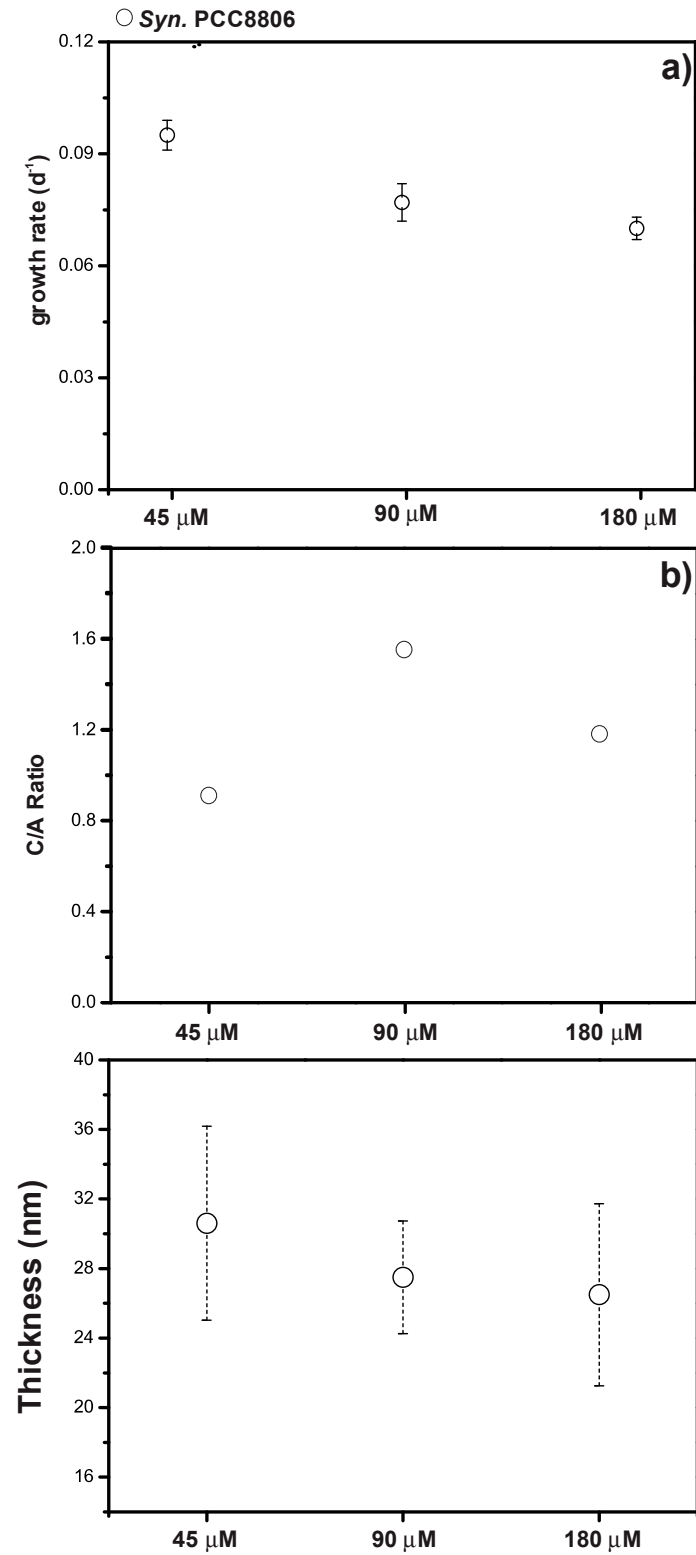


Figure S4. Variation of (a) the growth-rate constant (d^{-1}), (b) the C/A ratio and (c) the average thickness of Syn. PCC8806 under different P concentrations.

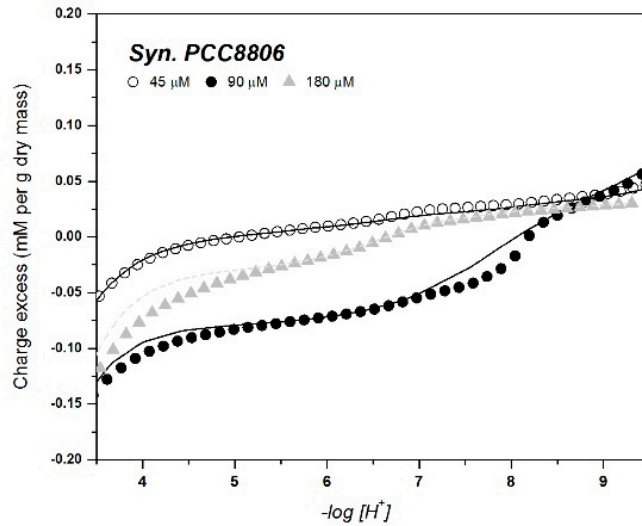


Figure S5. The results of the potentiometric titrations. The circles plots represent the average of three potentiometric titration for each strain and P condition. Fitted charge excess, see the formula (1) in the main text, obtained by LPM is represent by lines (dashed and continuous) with the same color as the corresponding P conditions.

Supplementary information 4. High-resolution XPS spectra

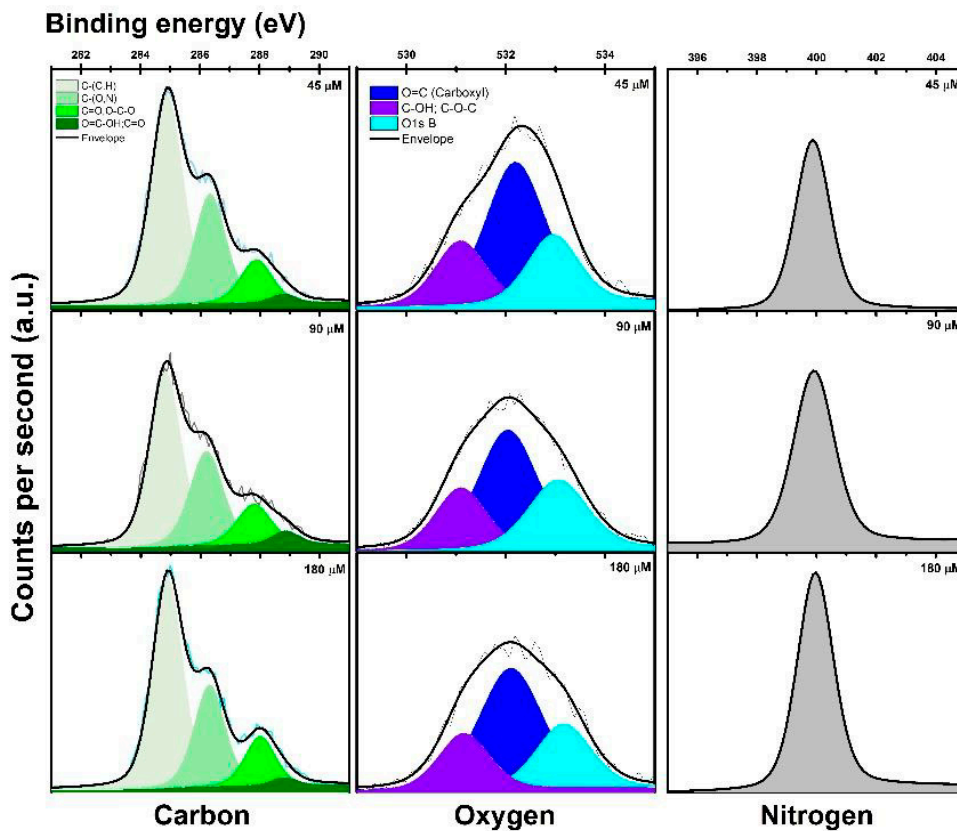
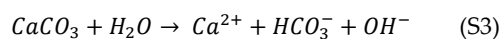
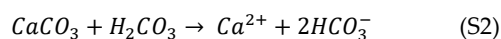
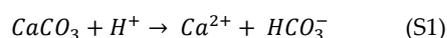


Figure S6. High resolution (0.1 eV step-size) XPS spectra of *Synechococcus* PCC8806 deconvoluted to C1s, O1s and N1s peaks to determined their chemistry.

Supplementary information 5. PhreeQc information

Carbonate kinetics was estimated according to the model defined by a rate equation (r) that assumes both dissolution (rf) and precipitation (rb) reactions and is defined by:



$$r = rf - rb = k_1[H^+] + k_2[H_2CO_3] + k_3[H_2O] - k_4[Ca^{2+}][HCO_3^-], \text{ in mmol/cm}^2/\text{s}$$

and where k1, k2, k3 and k4 are rate constants fitted to the experimental data as function of temperature (see [1] for more details).

Supplementary Information 6. Dynamics of dissolved calcium at different stages of biomineralization experiments

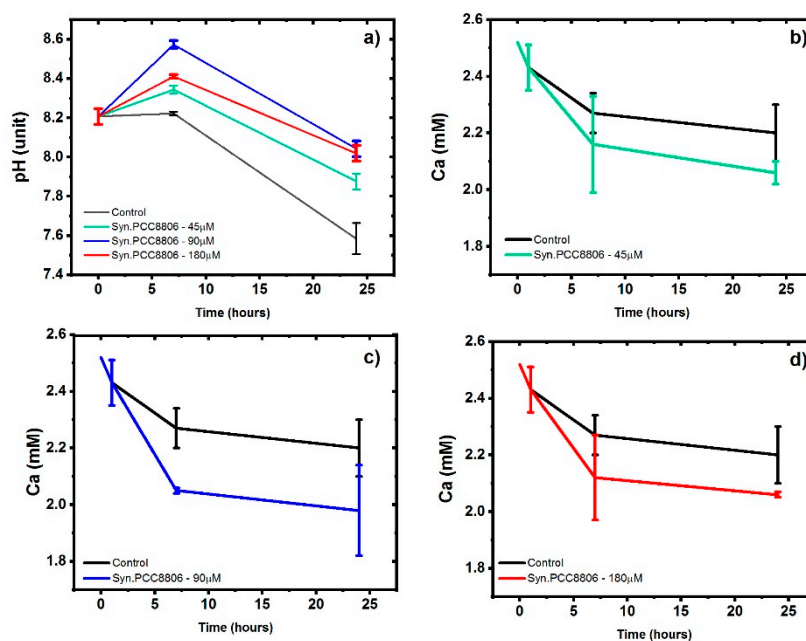


Figure S7. (a) Dynamics of pH in the abiotic (control) and in the presence of *Syn.* PCC8806 biomass. Data collected after 7 and 24 hours. (b), (c), and (d) dynamics of dissolved calcium at different stages of the experiment. The initial Ca concentration is 2.52mM.

Table S3. ANOVA analysis of Ca variation in precipitation experiments.

ANOVA: Control vs Syn. PCC8806-45µm						
Source of Variation	SS	df	MS	F	P-value	F crit
Between Groups	70.93	1	70.93	2.45	0.15	9.65
Within Groups	318.04	11	28.91			
Total	388.98	12				
ANOVA: Control vs Syn. PCC8806-90µm						
Source of Variation	SS	df	MS	F	P-value	F crit
Between Groups	233.0245	1	233.02	8.57	0.02	10.03
Within Groups	271.8527	10	27.19			

Total	504.8773	11				
ANOVA: Control vs Syn. PCC8806–180 μ m						
Source of Variation	SS	df	MS	F	P-value	F crit
Between Groups	101.2683	1	101.2683	1.899164	0.20	10.04
Within Groups	533.2256	10	53.32256			
Total	634.4939	11				

Supplementary Information 7. Correlation between the Ca removal rates, N content of surface cells and surface functional groups

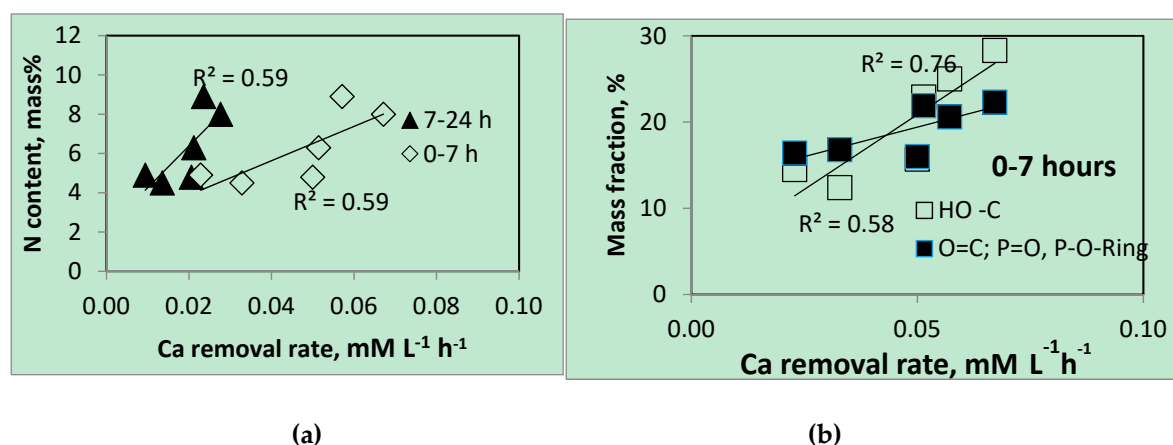


Figure S8. Ca removal rates and N content of cells surface (a) and surface functional groups (b)

Supplementary information 8 Principal component analysis of the FTIR spectra

Principal Component analysis of the FTIR spectra obtained at different pH during titrations revealed that the variance (>60%) of the dataset can be explained by the Principal component 1 (PC1) and 2 (PC2) score plots (Figure S9) of the standard normal variate transformation. This scaling method consisted of subtracting each row of the data set by its mean and dividing by the standard deviation [2]. The loading plots showed that bands associated with polysaccharide and protein regions largely control the sample variance (Figure S9). According to the PCA, the contribution of band regions associated with specific macromolecules strongly determined the cluster distribution of the spectra data (Figure S9). Syn. PCC8806-90 μ M functional group distribution is explained by PC1, and it is notorious the relevance of polysaccharides (1060 to 1100 cm^{-1}) and proteins (1555 and 1563 cm^{-1}) bands in the spectra, but also bands in the region between 1322 and 1360 cm^{-1} .

Although protein bands tend to dominate the spectra, we observed that the clusters of Syn. PCC8806-90 μ M and PCC8806-180 μ M were also aligned with the polysaccharide bands (900–1200 cm^{-1}). The score plot also indicates a higher relevance of phosphorus groups in Syn. PCC8806-180 μ M, which may be a related presence of P–OH and also the P–O–P vibrations of phosphate oligomers or glycosidic linkage ($\approx 923 \text{ cm}^{-1}$). On the other hand, the strong contribution of the protein region (1500–1700 cm^{-1}) both for the negative and, particularly, for the positive PC1 loading indicates that the deprotonation of the functional groups in this region is relevant for the process of biomineralization.

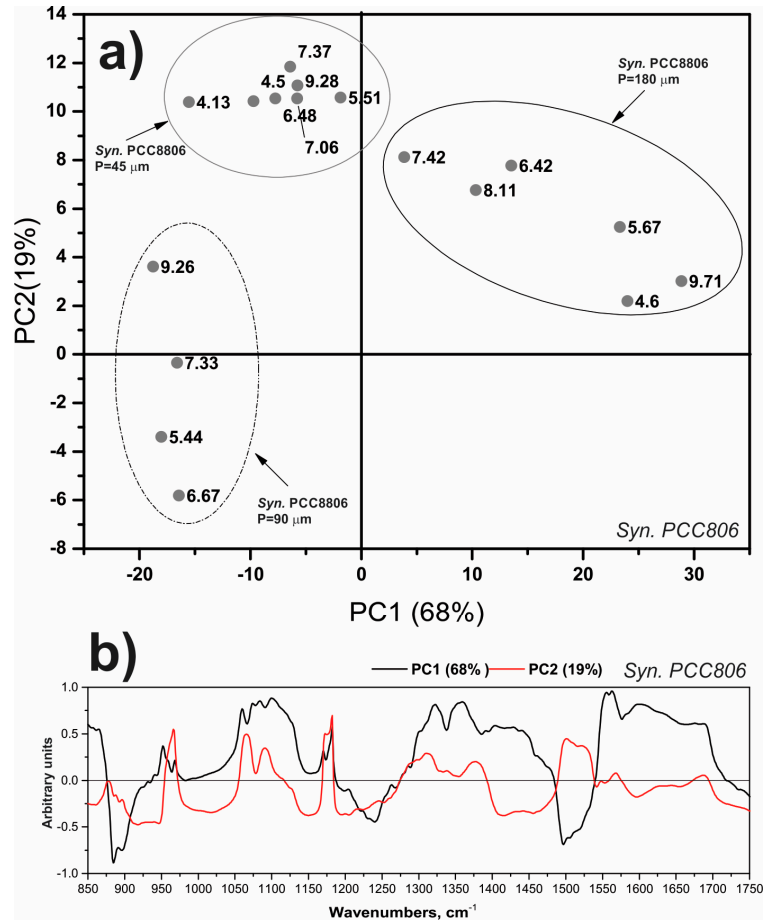
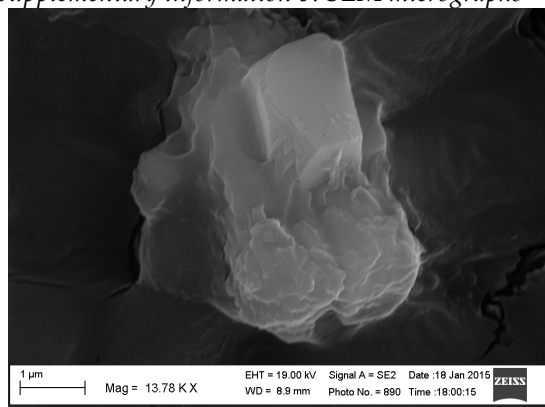
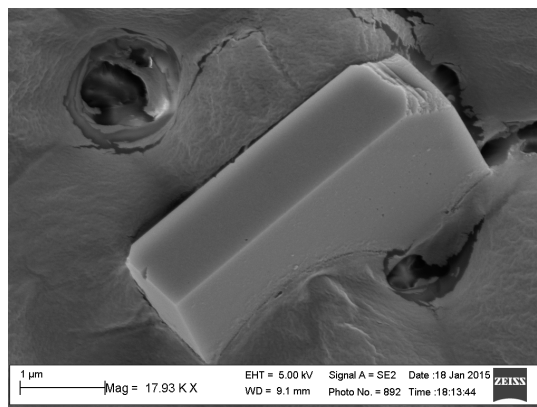


Figure S9. Principal components (PC1 vs. PC2) score plots (a) and loading plots (b) of the FTIR spectra of *Syn. PCC8806* obtained at different pH (indicated in the figure).

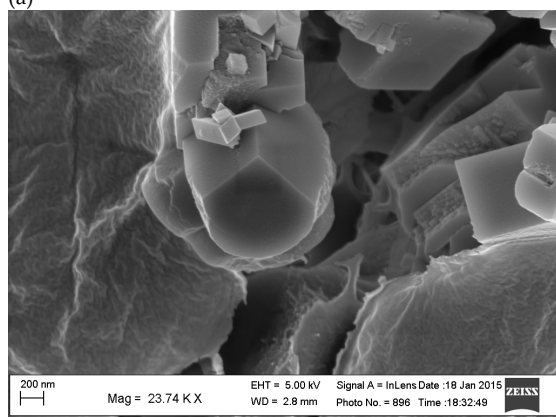
Supplementary information 9. SEM micrographs



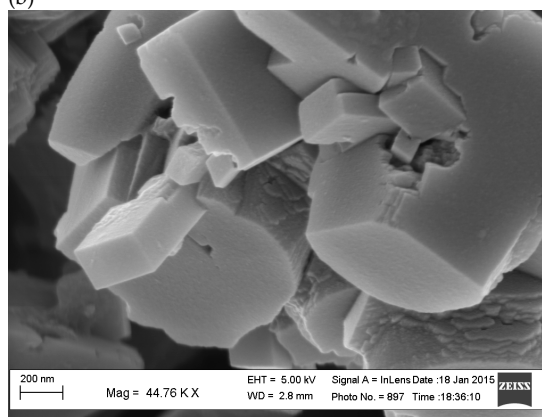
(a)



(b)



(c)



(d)

Figure S10. SEM micrographs of the precipitates (a-d) formed in the presence of cells Syn. PCC8806 cultured at 90 µM P.

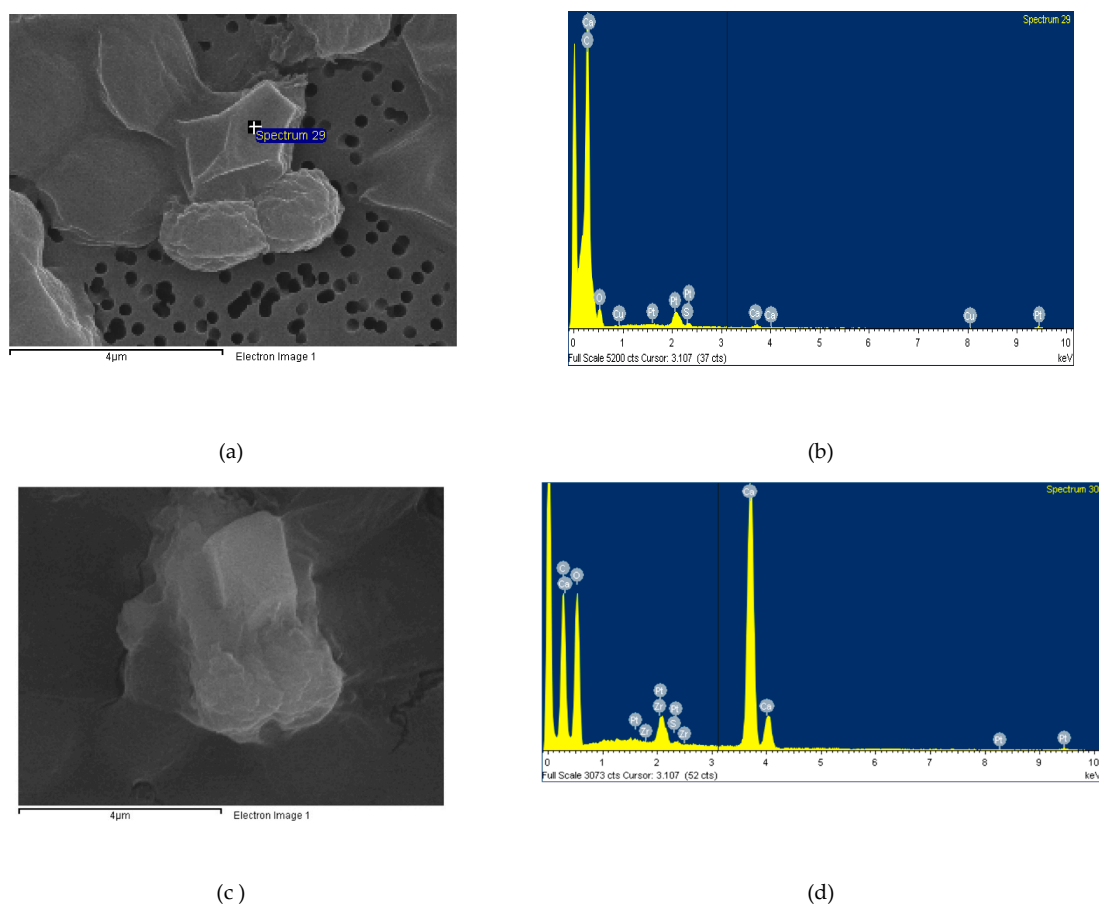


Figure S11. The SEM images and respective EDX spectra obtained from the precipitates in the biomineralization experiments; (a) and (b) with PCC8806-40 μ M; (c) and (d) with PCC8806-90 μ M

References

1. Appelo, C.A.J.; Postma, D. Carbonates and Carbon Dioxide. In *Geochemistry, Groundwater and Pollution*, Second Edition, 2nd edition ed.; Taylor & Francis: 2005; doi:10.1201/9781439833544.ch510.1201/9781439833544.ch5pp. 175-240.
2. Wehrli, P.M.; Lindberg, E.; Svensson, O.; Sparén, A.; Josefson, M.; Dunstan, R.H.; Wold, A.E.; Gottfries, J. Exploring bacterial phenotypic diversity using factorial design and FTIR multivariate fingerprinting. *Journal of Chemometrics* 2014, 28, S681-S686, doi:10.1002/cem.2588.



© 2018 by the authors. Submitted for possible open access publication under the terms and conditions of the Creative Commons Attribution (CC BY) license (<http://creativecommons.org/licenses/by/4.0/>)